Coupled effects of climate teleconnections on drought, Santa Ana winds and wildfires in southern California

Adrián Cardil [a,b,c,*], Marcos Rodrigues [d,e], Joaquin Ramirez [a], Sergio de-Miguel [b,c], Carlos A. Silva [f,g], Michela Mariani [h], Davide Ascoli [i]

[a] Technosylva Inc, La Jolla, CA, USA
[b] Department of Crop and Forest Sciences, University of Lleida, Lleida, Spain
[c] Joint Research Unit CTFC - AGROTECNIO, Solsona, Spain
[d] Department of Agricultural and Forest Engineering, University of Lleida, Lleida, Spain
[e] Institute University of Research in Sciences Environmental (IUCA), University of Zaragoza, Spain
[f] School of Forest Resources and Conservation, University of Florida, Gainesville, FL, USA
[g] Department of Geographical Sciences, University of Maryland, College Park, MD, USA
[h] School of Geography, University of Nottingham, Nottingham, UK
[i] Department of Agricultural, Forest and Food Sciences, University of Turin, Largo Braccini 2, 10095 Grugliasco, TO, Italy

HIGHLIGHTS

- Burned area is associated with adverse weather patterns in southern California.
- Climatic teleconnections play a key role in modulating fire-conducive conditions.
- Fire-promoting events are mediated by coupled effects of climate teleconnections.

GRAPHICAL ABSTRACT

ARTICLE INFO

ABSTRACT

Projections of future climate change impacts suggest an increase of wildfire activity in Mediterranean ecosystems, such as southern California. This region is a wildfire hotspot and fire managers are under increasingly high pressures to minimize socio-economic impacts. In this context, predictions of high-risk fire seasons are essential to achieve adequate preventive planning. Regional-scale weather patterns and climatic teleconnections play a key role in modulating fire-conducive conditions across the globe, yet an analysis of the coupled effects of these systems onto the spread of large wildfires is lacking for the region. We analyzed seven decades (1953–2018) of documentary wildfire records from southern California to assess the linkages between weather patterns and large-scale climate modes using various statistical techniques, including Redundancy Analysis, Superposed Epoch Analysis and Wavelet Coherence. We found that high area burned is significantly associated with the occurrence of adverse weather patterns, such as severe droughts and Santa Ana winds. Further, we document how these fire-promoting events are mediated by climate teleconnections, particularly by the coupled effects of *El Niño Southern Oscillation* and *Atlantic Multidecadal Oscillation*.

© 2020 Elsevier B.V. All rights reserved.

* Corresponding author at: Technosylva Inc, La Jolla, CA, USA.
E-mail address: adriancardil@gmail.com (A. Cardil).

1. Introduction

The interannual variability in both large wildfire occurrence and burned area is usually high in most ecosystems around the globe (Giglio et al., 2010). This phenomenon can be partially explained by the interaction between fire and annually-variable modes of sea surface temperature (SST) and related climate teleconnections (CTs; i.e. statistically significant climate remote responses far away from the forcing region, either concurrent with or time lagged; Kitzberger et al., 2007; Mariani et al., 2018, 2016; Schoennagel et al., 2005). However, these associations are not straightforward (Keeley, 2004) and underlying interactions among CTs may lead to specific modulations or amplifications (Ascoli et al., 2020; Wang et al., 2014) with varying effects on fire-prone weather patterns at subcontinental scales, subsequently influencing wildfire activity (Harris and Lucas, 2019). Under a climate change scenario projecting many regions on Earth towards an increase in number of wildfires (Moritz et al., 2012), understanding the effect of climate variability on large-wildfire occurrence is essential for an efficient long-term environmental resources planning, wildfire management and to properly forecast fire danger and risk during the fire season (Ramirez et al., 2019; Schoennagel et al., 2005).

The occurrence of drought, heat waves, high wind speed events and their combined effects are well-known contributing factors boosting fire danger in most fire-prone areas worldwide (Bowman et al., 2017; Cardil et al., 2019; Molina-Terrén and Cardil, 2016; Monedero et al., 2019). Such events may be mediated by SST modes such as *El Niño Southern Oscillation* (ENSO), the *Pacific Decadal Oscillation* (PDO), or the *Atlantic Multidecadal Oscillation* (AMO) and associated CTs, from interannual to multidecadal time scales (Kitzberger et al., 2006; Li et al., 2016; Molina-Terrén et al., 2016). CTs influence the atmosphere inducing cascading effects on local weather patterns across the globe (Chiodi and Harrison, 2015; Maleski and Martinez, 2018) and indirectly affect interannual variation in biomass production, vegetation phenological cycles and fuel moisture (Dannenberg et al., 2018; Kitzberger et al., 2017; Li et al., 2016).

To date, much research has been analyzing the links between CTs and seasonal weather conditions including effects on temperature, precipitation, evapotranspiration, soil moisture and drought (Abatzoglou and Kolden, 2013; Johnson and Wowchuk, 1993; O'Brien et al., 2019; Skinner et al., 2002; Turco et al., 2017; Westerling et al., 2006). The association between CTs and fire disturbance has also recently drawn considerable attention, especially in fire-prone regions (e.g. Australia, western United States), and strong evidence supports the existence of a link between CTs and burned area in many regions across the world (Aragão et al., 2018; Kitzberger et al., 2007; Mariani et al., 2018, 2016; Schoennagel et al., 2005). However, the interaction between CTs and their influence on burned area variability is difficult to unravel, since it depends on underlying modulations of the frequency, intensity and duration of specific weather events (Li et al., 2016). Moreover, the influence of CTs on burned area is non-stationary since the variability of the CT modes changes from interannual (ENSO) to multidecadal time periods (AMO and PDO) (Ascoli et al., 2020; Levine et al., 2017; Zanchettin et al., 2016).

Southern California is a wildfire hotspot in the western United States (Bowman et al., 2017), where the most destructive fires in its recorded history occurred in the 21st century, despite the increased wildfire suppression expenditures (Liang et al., 2008). It is well known that increases in wildfire activity in this region have been associated to high fuel dryness due to global warming exacerbation of evaporative demand (Williams et al., 2019), drought frequency and severity (Dettinger et al., 2011; Bond et al., 2015; Seager et al., 2015) and extreme winds in Autumn (Goss et al., 2020). The conjunction of subcontinental-scale patterns of drought spells and Santa Ana Winds (SAWs) affecting burned area variability might be modulated by CTs and their interactions. However, little is known about coupled effects of major climate modes influencing burned area in southern California

(Chikamoto et al., 2017; Keeley, 2004), and particularly in relationship to the local weather patterns promoting the largest wildfires in the region.

In this study, our aim was to disentangle the coupled effects of CTs and adverse weather conditions driving large wildfires across southern California during the last seven decades. Specifically, we address the following research objectives at different temporal windows: (1) To understand single and coupled effects of CTs in modulating the interannual variation of drought, SAWs, large wildfire activity and seasonal associations throughout the year; and (2) To examine the influence of decadal oscillations of CTs coupling on trends in burned area.

2. Methods

2.1. Study area

The study area was the Southern Coast Bioregion in California, USA, where wildfires have dramatically affected both forested lands and urban settlements in the past decades (Fig. 1). The region was defined based on the 9 bioregions outlined by Sugihara and Barbour (2006) who coalesced the 19 sections described by Miles and Goudey (1997) considering consistent patterns of vegetation and fire regime for whole California. The region is dominated by Mediterranean climatic conditions, known to foster recurrent large wildfires (Pyne et al., 1998). Fire-prone weather situations such as long and dry summers with thunderstorms episodes, low relative humidity and strong winds are typical of this region (Sugihara and Barbour, 2006).

2.2. Data

2.2.1. Wildfires

We used the Fire and Resource Assessment Program (FRAP) fire geodatabase from CAL FIRE which includes historical fire perimeters since 1878 (CAL FIRE, 2019) and represents the most complete record of medium and large fire data in California (Butry and Thomas, 2017). FRAP is developed by the US Forest Service Region 5, the Bureau of Land Management, the National Park Service, and CAL FIRE. The database includes timber fires greater than 0.04 km^2, shrub fires greater than 0.20 km^2, grass fires greater than 1.21 km^2, and those wildland fires that destroyed at least three structures or caused more than US\$ 300,000 in damage. Fires larger than 1.21 km^2 in all vegetation types in the period 1953–2018 were selected for further analysis in this study. The selected sample guarantees homogenous and complete fire event records for statistical analysis.

2.2.2. Climate teleconnections

In this paper, we addressed the effects of ENSO, AMO and PDO climate teleconnection signals on fire weather and activity in southern California from 1953 to 2018. One of the most prominent CTs having impact on California is the ENSO with a 3- to 7-year cycle between warm (El Niño) and cold (La Niña) phases (Yoon et al., 2015). We used the Oceanic Niño Index (ONI) [ERSST.v5 SST anomalies in the Niño 3.4 region (5° N to 5° S, 170° W to 120° W)], based on centered 30-year base periods updated every 5 years. The AMO is a long-term warming and cooling of North Atlantic SSTs with a cycle expanding over several decades (Enfield et al., 2001). The PDO is a Pacific climate teleconnection associated to changes in SST, sea level pressure, and wind patterns occurring in the northern Pacific Ocean causing widespread climatic variation over large areas of North America.

Data on all three CTs indexes was retrieved from the Climate Prediction Centre and the Earth System Research Laboratory of the National Oceanic and Atmospheric Administration (NOAA, 2019). The CT indexes were computed by averaging monthly values (6-month running average) from December to May, after testing all possible running averaging windows and month combinations, such as the widely used 3-month running mean for December, January and February. According to the literature,
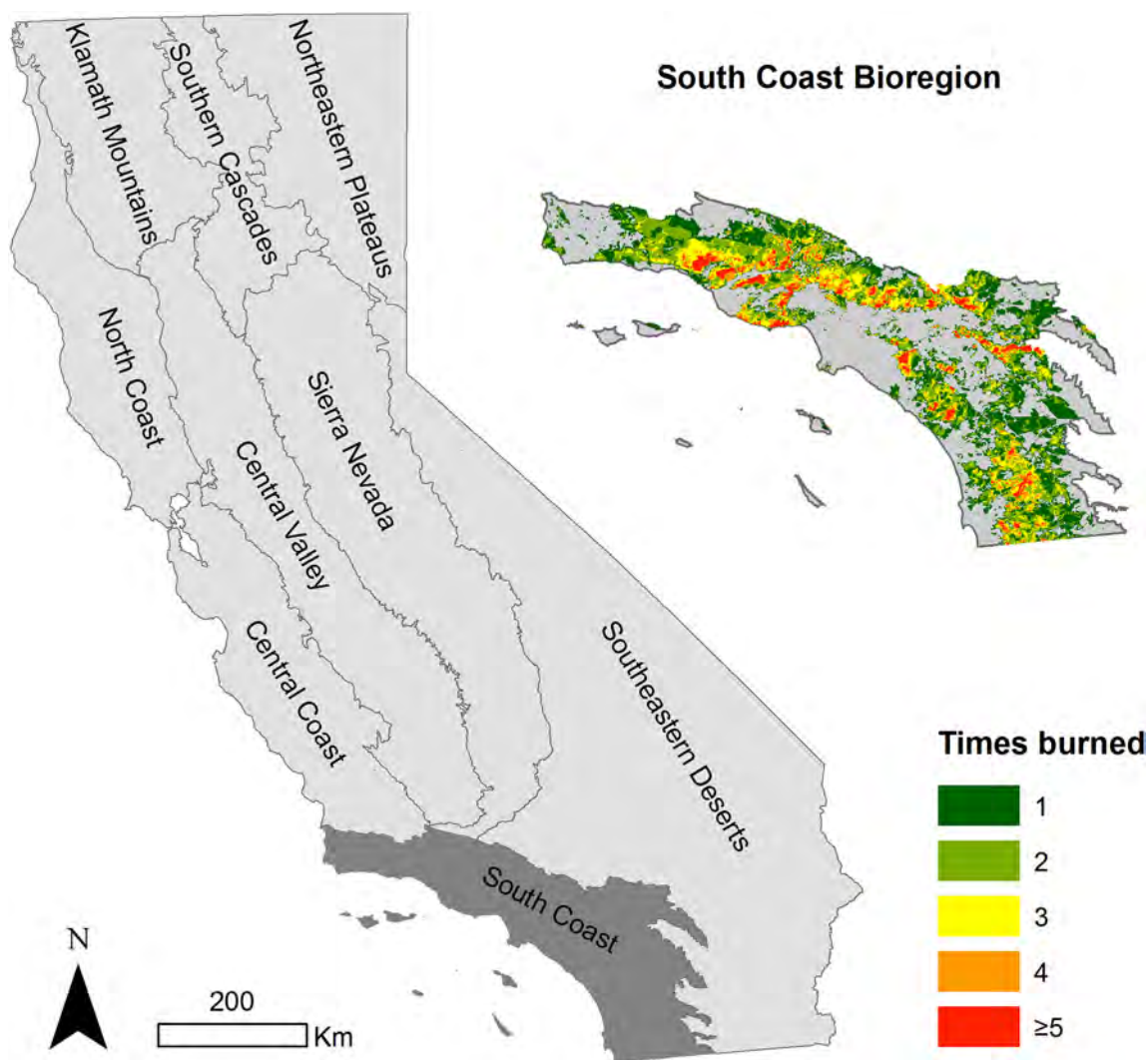
Fig. 1. Geographic location of the 9 bioregions delineated by Sugihara and Barbour (2006) including the fire-prone Southern Coast Bioregion in California with the times the landscape was burned across the study area in the study period (1953–2018) after superimposing all wildfire perimeters from CAL FIRE (2019) used in this analysis.

ENSO index may have the strongest relationships with fire activity in winter-spring months since it accounts for potential lagged effects on spring and summer drought (Shabbar and Skinner, 2004). This is especially relevant in a region where the window of storminess is narrow (typically between November and March), period during which most of the annual precipitation occurs (Cayan et al., 2016). To facilitate the analyses and interpretation of the findings, CTs were classified according to their positive and negative phases. Warm (ENSO > 0.5; El Niño), neutral (ENSO between −0.5 and 0.5) and cold (ENSO < −0.5; La Niña) periods for ENSO were classified based on a threshold of $+/-0.5$ °C. A warm or cold PDO/AMO phase corresponds to above or below zero values of the computed indexes, respectively. The temporal trend of the aforementioned indexes is shown in the supplementary materials (Figs. S1 and S2).

2.2.3. Drought data

To account for drought conditions, we used the Standardized Precipitation Evapotranspiration Index (SPEI), a multiscale drought index that represents a climatic water balance by combining precipitation and potential evapotranspiration. SPEI data were retrieved from the global SPEI database (v2.5), based on the FAO-56 Penman-Monteith estimation of potential evapotranspiration (Vicente-Serrano et al., 2017). The database compiles SPEI data spanning from 1 to 48 months at a spatial resolution of 0.5 degrees (1950–2015) and 1.0 degrees (2016–2018). A 12-month

accumulation period ($SPEI_{12}$) was considered to depict yearly drought anomalies ($SPEI_{12} < -0.85$), considering December as reference month. Previous works have found $SPEI_{12}$ as the best overall drought hazard indicator (Blauhut et al., 2016; Pai Mazumder et al., 2016).

2.2.4. Santa Ana wind data

We used the SAW dataset compiled by (Abatzoglou et al., 2013) available at http://nimbus.cos.uidaho.edu/JFSP/pages/publications. html from 1950 to present. Days with SAW conditions (SAD) were classified considering the criteria of a northeast–southwest sea level pressure gradient across southern California, and a strong cold air advection from the desert into the Transverse Range through daily data from the NCEP/NCAR Reanalysis dataset (Kalnay et al., 1996). We chose this dataset because it is representative for the study area, covers a longer period compared to other SAW datasets and has been validated with actual SAW events in the National Climatic Data Center storm database (Li et al., 2016).

2.3. Statistical analysis

We performed several statistical analyses to (i) assess the relationships between CTs, weather patterns (SPEI and SAD) and fire incidence (burned area and fire size), and test the significance and magnitude of

the observed relationships, and (ii) explore time-dependent associations between the aforementioned variables at seasonal, inter-annual, and decadal levels. Redundancy analysis (RDA) was performed to analyze the association of the aforementioned variables at seasonal and inter-annual scales; Superposed Epoch Analysis (SEA) was used to analyze lagged CT effects on burned area; Multigroup comparison tests were conducted to assess differences in fire size distribution and annual burned area among the different phases of CTs; and wavelet coherence analysis to identify coupled effects of CTs on trends in burned area at decadal time scales.

All statistical analyses and tests were conducted using the R software (R core development team, 2017) with a confidence level of 95% (P < 0.05).

2.3.1. Redundancy analysis

A RDA was used to investigate potential associations between CTs, weather conditions (SPEI$_{12}$ and annual number of SAD) and burned area seasonally. Redundancy analysis is a multivariate approach widely used to model the association of a set of response variables to different explanatory factors. Similar to Principal Component Analysis (PCA), RDA decomposes the information into several dimensions depicting independent association patterns. Contrary to PCA, RDA allows specifying multiple variables as response, so that new dimensions portray the degree of association between the input driving factors and the targeted responses. More details about the technique can be found in Legendre and Legendre (2012). The significance of the effect of constraints was analyzed through an ANOVA permutation test. RDA was conducted using the *vegan* R package (Oksanen et al., 2019).

2.3.2. Superposed Epoch Analysis

A SEA (dplR package (Bunn et al., 2019)) was used to determine the significance of the departure from the mean and lagged years in terms of burned area for the different phases of the studied CTs through bootstrapped confidence intervals (Lough and Fritts, 1987) for a given set of key event years during the 1953–2018 period. We analyzed the effect of ENSO on lagged burned area considering both La Niña and El Niño years as events. Also, we tested its interaction with cold and hot phases of AMO and PDO. Given that both PDO and AMO show decadal oscillations, and SEA requires annually-resolved data, we only included these modes in the SEA analysis in combination with ENSO (i.e., selecting as events those years with La Niña/El Niño and positive/negative AMO or PDO phases).

2.3.3. Multigroup comparison tests

The further step of our analysis aimed at detecting differences in fire size distribution and annual burned area among the different phases of CTs. We applied the multiple comparison test with unequal sample sizes by Kruskal and Wallis (Kruskal and Wallis, 1952) and a posteriori Dunn's test (Dunn, 1964) with *Bonferroni* correction. The $H_1 > H_0$ hypothesis, indicates whether there is a statistical significance in fire size and annual burned area between any specific coupled CTs. Fire events were split among different coupled combinations of CTs phases (ENSO+/ENSO-, AMO+/AMO- and PDO+/PDO-), dry versus wet conditions and the presence/absence of SAW (fire activity during SAD and fire activity in no SAD). The resulting groups were submitted to the Dunn's test using fire size and burned area.

2.3.4. Wavelet coherence analysis

A final analysis aimed at testing for decadal influences of CTs on trends in seasonal burned area. We used a wavelet coherence analysis to measure the intensity of the covariance of CTs and burned area patterns in the time-frequency space throughout the study period (Ascoli et al., 2020; Mariani et al., 2016). The test allows the detection of time-localized common oscillatory behavior of non-stationary signals through a cross-correlation between two time series as a function of time and frequency. In particular, to account for the coupled effect of CTs, we

computed a combined index by running a PCA of AMO and ENSO. The PCA-eigenvector indicative of the alignment of AMO+ and ENSO- phases was selected and yearly scores of the component used to test the wavelet coherence with the yearly burned area in spring-summer. The analysis was carried out using the R package *biwavelet* (Gouhier et al., 2016) using a Morlet continuous wavelet transform and considering the lag −1 autocorrelation of each series. The data were padded with zeros at each end to reduce wraparound effects. Significance of coherence at all frequencies lower than two years was tested using a time-average test with 2000 Monte Carlo randomizations.

3. Results

3.1. Climate teleconnections, drought and Santa Ana winds

The RDA analysis revealed interesting associations between CTs and fire-prone weather patterns (drought and annual number of SAD; Fig. 2). Drought, represented by the SPEI$_{12}$ index, was positively correlated with ENSO (P < 0.01), with higher drought conditions during La Niña phases than during El Niño events. The positive phase of AMO tended to be related with a higher annual number of SAD, but the relationship was not statistically significant (P = 0.11). PDO was not significantly correlated to either SPEI$_{12}$ or SAD.

We detected synchrony between drought conditions and the annual number of SAD (Figs. 2, S1 and S2), so that larger annual burned areas occurred in those periods with coincident drought and SAW conditions (average annual burned area of 54,489 ha considering the 1983–1993 and 2002–2018 periods vs 39,030 ha for the rest of years; P < 0.01; see Fig. S1).

3.2. Burned area, fire size and climate teleconnections

A total of 1412 unplanned fires larger than 1.21 km^2 burned a total area of 2,995,092 ha in the study area during the period
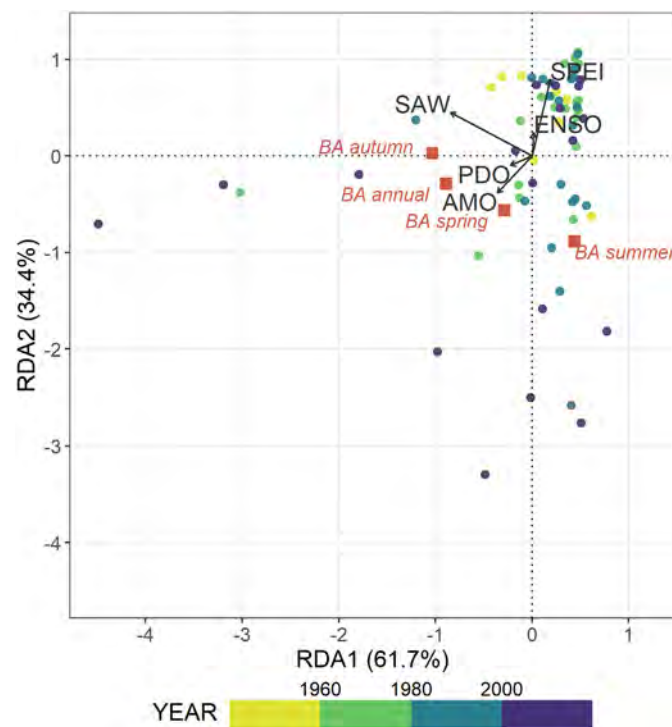

Fig. 2. Redundancy analysis (RDA) bi-plot (1953–2018). Points show annual scores, vectors show climate teleconnection (AMO, PDO and ENSO), drought (SPEI$_{12}$) and Santa Ana wind (SAW) parameters and red marks represent the response variables: burned area (BA) in autumn, summer, spring and annual. (For interpretation of the references to colour in this figure legend, the reader is referred to the web version of this article.)

1953–2018, with an average fire size of 2121 ± 182 ha (standard error). The annual burned area was significantly larger under the positive phase of AMO (P = 0.049; Fig. 3A). A similar trend was found with PDO-, though statistically non-significant (P = 0.075; Fig. 3C). The SEA analysis revealed non-significant temporal relationships between annual burned area and the cold (La Niña) and warm (El Niño) phases of ENSO at any annual time lag, even though the SPEI$_{12}$ index was significantly correlated with ENSO as shown by the RDA analysis. However, based on the SEA analysis we found a significant synchronous effect between AMO+ and El Niño, resulting in larger annual burned area (time lag = 0 years; P = 0.04), as shown in Fig. 3A.

The combined influence of SPEI$_{12}$ and SAW on both total burned area and median fire size was significant (P < 0.01), being their effects modulated by certain CTs modes. A large fraction area (80%) was burned under drought or SAW episodes. The portion of area burned under drought and SAWs was meaningfully dissimilar depending on the CTs phases. The largest fraction of burned area occurred under the conjunction of ENSO+, AMO+, drought and SAW conditions (Fig. 3), with almost no influence of PDO. During El Niño period, the differences in burned area under SAW and non-SAW conditions were small, whereas during La Niña most of the burned area occurred under non-SAW conditions (75%). The burned area under La Niña was more closely associated with drought conditions (83.4%) compared to El Niño period
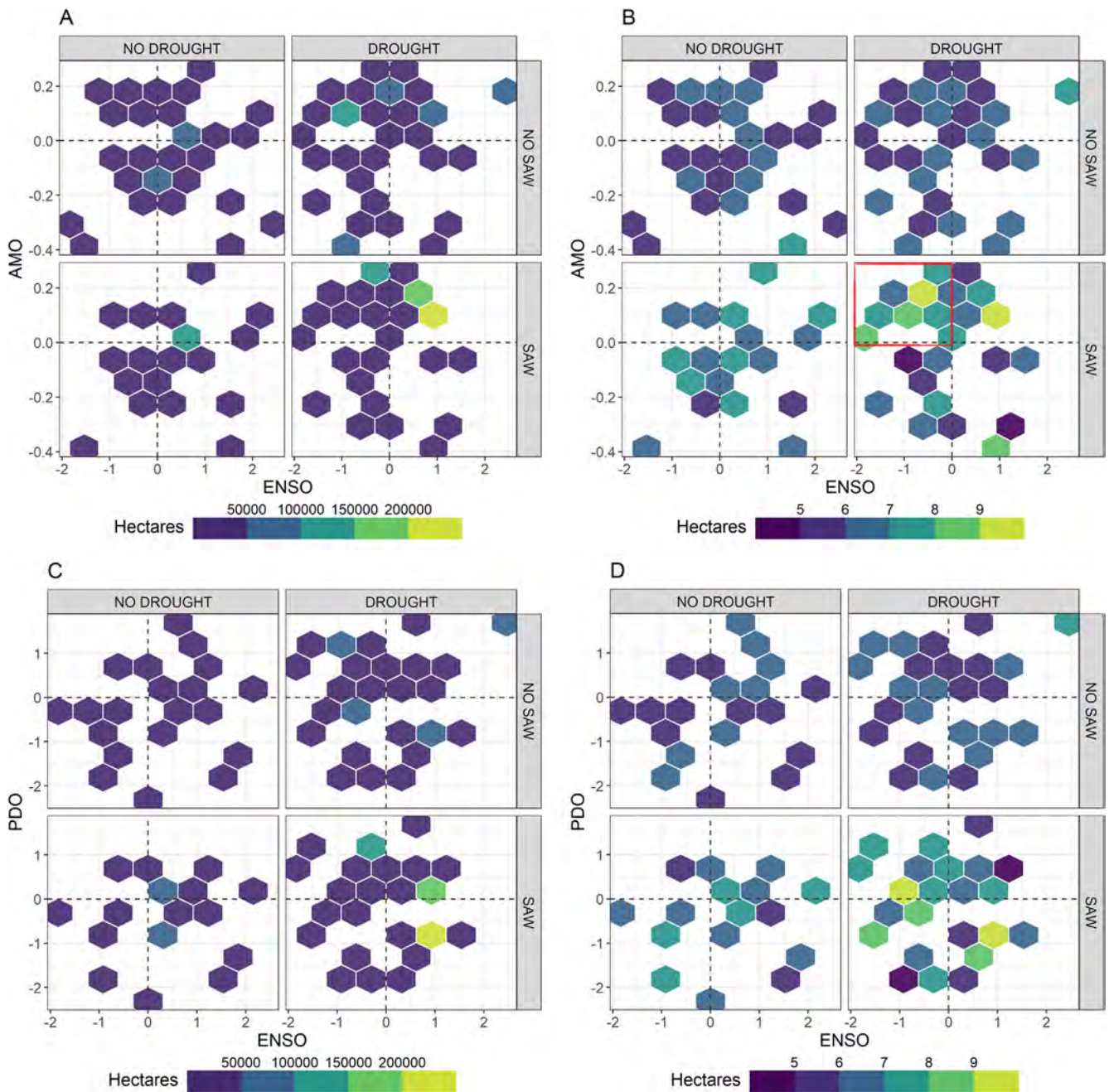

Fig. 3. Sum of burned area (pannels A and C) and median fire size (log-transformed; pannels B and D) for each combination of CTs (AMO, PDO and ENSO), SAW and drought (SPEI$_{12}$). The highlighted pannel in red represents larger median fire size during La Niña, AMO+, SAW and drought conditions compared to other combinations. (For interpretation of the references to colour in this figure legend, the reader is referred to the web version of this article.)

(64.2%). Also, the distribution of burned area was asymmetrically negative for ENSO, with most fires occurring when ENSO was lower than 1 (Fig. 3). The percentage of burned area in SAD and under drought conditions was higher for AMO+ than AMO-. The PDO followed a different pattern, with higher proportion of burned area under PDO- in those fires occurring under SAW and PDO+ under drought conditions.

Fires were usually larger under SAW (P < 0.001) and drought conditions (P < 0.01), particularly in coincident drought and SAW situations (P < 0.01; Fig. 3B and D). The median fire size was significantly larger during the positive phase of AMO compared to its negative phase (P = 0.011). Also, those fires that occurred under AMO+ and SAD were larger than those occurring under AMO- or non-SAD (P < 0.01). These relationships between CT phases and fire size did not occur under PDO and ENSO.

3.3. Seasonal burned area variability

We found noteworthy seasonal differences in burned area modulated by CT modes and weather patterns (Fig. 2). The area burned in autumn was significantly linked to SAW conditions (P < 0.01) while the burned area in summer, and especially in spring, was significantly linked to drought (P = 0.03). The association between AMO and annual burned area was close to the chosen significance threshold in the RDA analysis (P = 0.059, threshold: P < 0.05), attaining similar p-values to the SEA analysis. Most of the burned area during autumn occurred under AMO+, SAW and mainly in combination with El Niño (Fig. S3). The effect of PDO was non-significant (P = 0.11).

Despite the significant link between SPEI and ENSO, the association between ENSO and burned area was not significant in any season, as obtained from the SEA analysis.

The Wavelet coherence analysis between the combined CTs index (AMO+/ENSO-) and burned area in summer and spring from 1953 to 2018 showed a significant coherence (Fig. 4), which shifted from a period domain of 8 years between 1960 and 1980 to a frequency of 2–6 years in more recent decades (red regions with black contours in the graph). In these periods, wavelet coherence showed an in-phase

fluctuation (i.e., the two time series move in the same direction) between the CTs coupled index and burnt area (arrows pointing right) with AMO+/ENSO- mostly leading the oscillation (arrows pointing down).

4. Discussion

This study contributes to disentangling the effect of the main CTs and their relations with local weather events such as drought and SAW in driving wildfire incidence (i.e., fire size and annual burned area) in southern California, by analyzing historical wildfires over the last 70 years. Our work confirms the importance of adverse weather conditions (i.e., drought and SAW) to explain burned area seasonally in southern California (Goss et al., 2020), and reveals that these relationships are mediated by CTs. The SPEI index was significantly correlated to ENSO positively, with wetter conditions found during El Niño years (Gergis and Fowler, 2009) due to increased precipitation in southern California (Allen and Anderson, 2018). This pattern may explain the seasonal burned area variability shown in this paper between the two phases of ENSO, as larger burned areas were also identified during drier La Niña years in the southwestern United States (Mason et al., 2017). While wildfires tended to occur during La Niña events under drought conditions, especially in spring and summer (Kitzberger et al., 2007), during El Niño phases a substantial number of large wildfires burned during SADs in autumn. This finding is probably related to plant growth and fuel accumulation with higher development of biomass under wetter conditions in the preceding spring (Westerling et al., 2003).

The warm phase of AMO is associated with decreased precipitation and increased mean temperature in western United States. These conditions probably boosted larger annual burned area as showed the SEA and RDA analysis. Also, the patterns of interannual rainfall variability associated with ENSO are significantly modulated between AMO phases. Enfield et al. (2001) found an increased positive correlation between ENSO and rainfall in southern California during the negative phase of AMO (1965–1994) as compared to its positive phase (1930–1959).
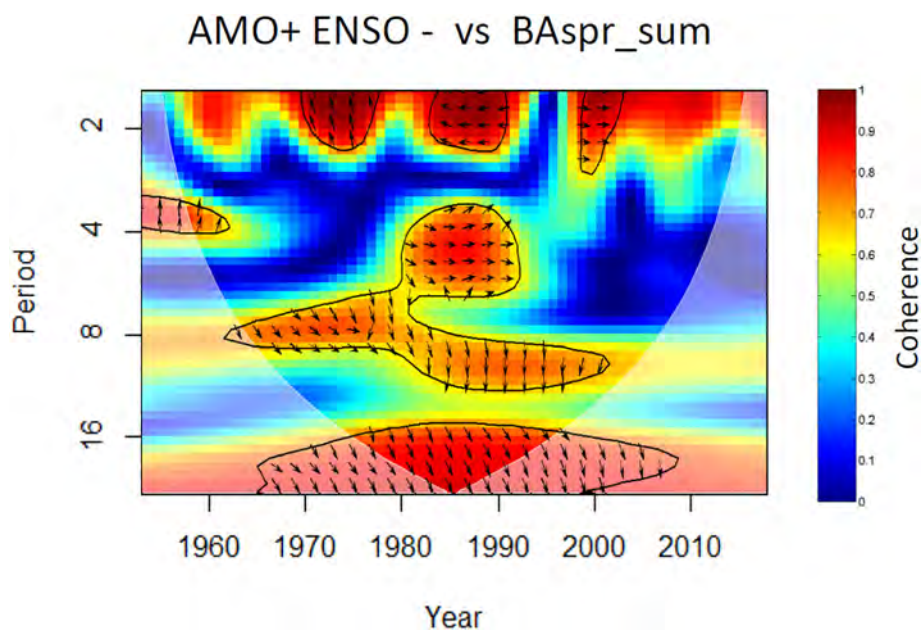

Fig. 4. Wavelet coherence between the combined teleconnection index (AMO+/ENSO-) and burned area (spring and summer) in Southern California. The test analyzes the coupled effect of positive AMO and the cool ENSO phase (La Niña) on the burnt area. Areas of strong coherence in time between series are shown in red. Black contours designate frequencies of significant coherence (p < 0.05, two-sided test) against red noise. Lighter shading shows the cone of influence where edge effects are important. Arrows pointing right show an in-phase behavior and arrows pointing down indicate a lead of the combined teleconnection index over the burned area. (For interpretation of the references to colour in this figure legend, the reader is referred to the web version of this article.)

This effect may explain the interaction found between AMO+, El Niño and annual burned area in the SEA analysis. In addition, the wavelet coherence analysis showed that the coupled AMO+/ENSO- index displayed a common non-stationary oscillation with the burnt area in spring and summer in southern California with periods ranging from 8 to 4 years, indicative of an amplification of La Niña during AMO+ phases with cascading effects on the fire regime.

Although we did not find any significant relationship between PDO, weather and fire activity, PDO may have a modulating effect on the climate patterns resulting from ENSO based on recent literature (Abiy et al., 2019; Margolis and Swetnam, 2013; Schoennagel et al., 2005; Wang et al., 2014). Wang et al. (2014) found that the climate signal of La Niña is likely to be stronger when PDO is highly negative, resulting in dry conditions in southern California; and, oppositely, highly positive PDO values would lead to El Niño-like wet conditions. Margolis and Swetnam (2013) found that ENSO influenced variability in moisture and upper elevation fire occurrence in the southwestern United States, and that such relationship could be potentially modulated by phases of PDO.

The RDA analysis suggests that the response of burned area to drought and SAW conditions is stronger in the 21st century compared to the second half of the 20th century, for fires occurring in the autumn under SADs and in summer with severe drought. This could be explained by the higher frequency of drought and SAW events in the 2000–2018 period, with AMO in its warm phase and PDO in its cool phase (Fig. S1 and S2), coupled with improved fire suppression capabilities (Liang et al., 2008) where only a few fires under extreme circumstances exceeded the initial attack and become large.

5. Conclusion

Our results highlight the coupled impacts of CTs on weather and burned area at both inter-annual and decadal time scales in Southern California. When using ENSO-based forecasts at seasonal scale, our findings reveal the need for considering the interaction with AMO. ENSO activity is projected to amplify due to anthropogenic climate change (Cai et al., 2014, 2015; Power et al., 2013), heralding a serious threat the ever expanding flammable rural-urban interface in this wildfire hotspot (Bowman et al., 2017). Since AMO is projected to enter a negative phase during the next decades (Krokos et al., 2019), this could limit the strength of La Niña phases conducive to fire-prone weather and spring-summer burnt area. In light of future climate change pressures, we suggest that proper drought monitoring (through indexes such as SPEI) and SAD forecasting is needed to gauge the very beginning of dry periods, and by extent, the prediction of high-risk fire seasons to further assist decision makers.

Supplementary data to this article can be found online at https://doi.org/10.1016/j.scitotenv.2020.142788.

CRediT authorship contribution statement

A.C., M.R., and D.A. conceived the ideas and designed methodology; A.C collected the data; A.C., M.R., and D.A. analyzed the data; and A.C. led the writing of the manuscript with contribution from all co-authors. M.R., J.R., S.d-M., C. S. and D.A., finally all co-authors contributed critically to the drafts and gave final approval for publication.

Declaration of competing interest

The authors declare that there is no conflict of interest.

References

Abatzoglou, J., Kolden, C., 2013. Relationships between climate and macroscale area burned in the western United States. Int. J. Wildl. Fire 22, 1003–1020.

Abatzoglou, J.T., Barbero, R., Nauslar, N.J., 2013. Diagnosing Santa Ana winds in Southern California with synoptic-scale analysis. Weather Forecast. 28, 704–710. https://doi.org/10.1175/waf-d-13-00002.1.

Abiy, A.Z., Melesse, A.M., Abtew, W., 2019. Teleconnection of regional drought to ENSO, PDO, and AMO: Southern Florida and the Everglades. Atmosphere (Basel) 10, 1–15. https://doi.org/10.3390/atmos10060295.

Allen, R.J., Anderson, R.G., 2018. 21st century California drought risk linked to model fidelity of the El Niño teleconnection. npj Clim. Atmos. Sci. 1, 21. https://doi.org/10.1038/s41612-018-0032-x.

Aragão, L.E.O.C., Anderson, L.O., Fonseca, M.G., Rosan, T.M., Vedovato, L.B., Wagner, F.H., Silva, C.V.J., Silva Junior, C.H.L., Arai, E., Aguiar, A.P., Barlow, J., Berenguer, E., Deeter, M.N., Domingues, L.G., Gatti, L., Gloor, M., Malhi, Y., Marengo, J.A., Miller, J.B., Phillips, O.L., Saatchi, S., 2018. 21st Century drought-related fires counteract the decline of Amazon deforestation carbon emissions. Nat. Commun. 9, 536. https://doi.org/10.1038/s41467-017-02771-y.

Ascoli, D., Hacket-Pain, A., LaMontagne, J.M., Cardil, A., Conedera, M., Maringer, J., Motta, R., Pearse, I.S., Vacchiano, G., 2020. Climate teleconnections synchronize Picea glauca masting and fire disturbance: evidence for a fire-related form of environmental prediction. J. Ecol. 108, 1186–1198. https://doi.org/10.1111/1365-2745.13308.

Blauhut, V., Stahl, K., Stagge, J.H., Tallaksen, L.M., De Stefano, L., Vogt, J., 2016. Estimating drought risk across Europe from reported drought impacts, drought indices, and vulnerability factors. Hydrol. Earth Syst. Sci. 20, 2779–2800. https://doi.org/10.5194/hess-20-2779-2016.

Bond, N.A., Cronin, M.F., Freeland, H., Mantua, N., 2015. Causes and impacts of the 2014 warm anomaly in the NE Pacific. Geophys. Res. Lett. 42, 3414–3420. https://doi.org/10.1002/2015GL063306.

Bowman, D.M.J.S., Williamson, G.J., Abatzoglou, J.T., Kolden, C.A., Cochrane, M.A., Smith, A.M.S., 2017. Human exposure and sensitivity to globally extreme wildfire events. Nat. Ecol. Evol. 1, 58.

Bunn, S., Korpela, M., Biondi, F., Campelo, F., Mérian, P., Qeadan, F., Zang, C., 2019. dplR: Dendrochronology Program Library in R. R Package Version 1.7.0.

Butry, D.T., Thomas, D.S., 2017. Underreporting of wildland fires in the US Fire Reporting System NFIRS: California. Int. J. Wildl. Fire 26, 732–743.

Cai, W., Borlace, S., Lengaigne, M., van Rensch, P., Collins, M., Vecchi, G., Timmermann, A., Santoso, A., McPhaden, M.J., Wu, L., England, M.H., Wang, G., Guilyardi, E., Jin, F.-F., 2014. Increasing frequency of extreme El Niño events due to greenhouse warming. Nat. Clim. Chang. 4, 111–116 Online: https://doi.org/10.1038/nclimate2100.

Cai, W., Wang, G., Santoso, A., McPhaden, M.J., Wu, L., Jin, F.-F., Timmermann, A., Collins, M., Vecchi, G., Lengaigne, M., England, M.H., Dommenget, D., Takahashi, K., Guilyardi, E., 2015. Increased frequency of extreme La Niña events under greenhouse warming. Nat. Clim. Chang. 5, 132–137 Online: https://doi.org/10.1038/nclimate2492.

CALFIRE, 2019. FRAP mapping [WWW document]. URL. http://frap.fire.ca.gov/data/frapgisdata-sw-fireperimeters_download (accessed 5.17.19).

Cardil, A., Vega-garcía, C., Ascoli, D., Molina-terrén, D.M., Silva, C.A., Rodrigues, M., 2019. How does drought impact burned area in Mediterranean vegetation communities ? Sci. Total Environ. 693, 133603. https://doi.org/10.1016/j.scitotenv.2019.133603.

Cayan, D., Dettinger, M., Pierce, D., Das, T., Knowles, N., Ralph, F., Sumargo, E., 2016. Natural variability, anthropogenic climate change, and impacts on water availability and flood extremes in the western United States. In: Miller, K., Hamlet, A., Kenney, D., Redmont, K. (Eds.), Water Policy and Planning in a Variable and Changing Climate. Taylor & Francis, p. 419.

Chikamoto, Y., Timmermann, A., Widlansky, M.J., Balmaseda, M.A., Stott, L., 2017. Multi-year predictability of climate, drought, and wildfire in southwestern North America. Sci. Rep. 7, 6568. https://doi.org/10.1038/s41598-017-06869-7.

Chiodi, A.M., Harrison, D.E., 2015. Global seasonal precipitation anomalies robustly associated with El Niño and La Niña events—an OLR perspective. J. Clim. 28, 6133–6159. https://doi.org/10.1175/JCLI-D-14-00387.1.

Dannenberg, M.P., Wise, E.K., Janko, M., Hwang, T., Smith, W.K., 2018. Atmospheric teleconnection influence on North American land surface phenology. Environ. Res. Lett. 13. https://doi.org/10.1088/1748-9326/aaa85a.

Dettinger, M.D., Ralph, F.M., Das, T., Neiman, P.J., Cayan, D.R., 2011. Atmospheric rivers, floods and the water resources of California. Water 3, 445–478. https://doi.org/10.3390/w3020445.

Dunn, O., 1964. Multiple comparisons using rank sums. Technometrics 6, 241–252.

Enfield, D.B., Mestas-nunez, A.M., Trimble, P.J., 2001. The Atlantic Multidecadal Oscillation and its relation to rainfall and river flows in the continental U.S. The Atlantic multidecadal oscillation and its relation to rainfall and river flows in the continental U.S. Geophys. Res. Lett. 28, 2077–2080. https://doi.org/10.1029/2000GL012745.

Gergis, J., Fowler, A., 2009. A history of ENSO events since AD 1525: implications for future climate change. Clim. Chang. 92, 343–387.

Giglio, L., Randerson, J.T., Van Der Werf, G.R., Kasibhatla, P.S., Collatz, G.J., Morton, D.C., Defries, R.S., Space, R., Sciences, E., Carolina, N., Biology, E., 2010. Assessing variability and long-term trends in burned area by merging multiple satellite fire products. Biogeosciences 7, 1171–1186.

Goss, M., Swain, D.L., Abatzoglou, J.T., Sarhadi, A., Kolden, C., Williams, A.P., Diffenbaugh, N.S., 2020. Climate change is increasing the risk of extreme autumn wildfire conditions across California. Environ. Res. Lett. https://doi.org/10.1088/1748-9326/ab83a7.

Gouhier, T.C., Grinstead, A., Simko, V., 2016. Biwavelet: Conduct Univariate and Bivariate Wavelet Analyses (Version 0.20.10).

Harris, S., Lucas, C., 2019. Understanding the variability of Australian fire weather between 1973 and 2017. PLoS One 14, e0222328.

Johnson, E.A., Wowchuk, D.R., 1993. Wildfires in the southern Canadian Rocky Mountains and their relationship to mid-tropospheric anomalies. Can. J. For. Res. 23, 1213–1222.

Kalnay, E., Kanamitsu, M., Kistler, R., Collins, W., Deaven, D., Gandin, L., Iredell, M., Saha, S., White, G., Woollen, J., Zhu, Y., Chelliah, M., Ebisuzaki, W., Higgins, W., Janowiak, J., Mo, K.C., Ropelewski, C., Wang, J., Leetmaa, A., Reynolds, R., Jenne, R., Joseph, D., 1996. The NCEP/NCAR 40-year reanalysis project. Bull. Am. Meteorol. Soc. 77, 437–472. https://doi.org/10.1175/1520-0477(1996)077<0437:TNYRP>2.0.CO;2.

Keeley, J.E., 2004. Impact of antecedent climate on fire regimes in coastal California ∗. Int. J. Wildl. Fire 13, 173–182.

Kitzberger, T., Brown, P.M., Heyerdahl, E.K., Swetnam, T.W., Veblen, T.T., 2006. Contingent Pacific – Atlantic Ocean Influence on Multicentury Wildfire Synchrony Over Western North America.

Kitzberger, T., Brown, P.M., Heyerdahl, E.K., Swetnam, T.W., Veblen, T.T., 2007. Contingent Pacific – Atlantic Ocean influence on multicentury wildfire synchrony over western North America. Proc. Natl. Acad. Sci. 104, 543–548.

Kitzberger, T., Falk, D.A., Westerling, A.L., Swetnam, T.W., 2017. Direct and indirect climate controls predict heterogeneous early-mid 21 st century wildfire burned area across western and boreal North America. PLoS One 12, e0188486. https://doi.org/10.1371/journal. pone.0188486.

Krokos, G., Papadopoulos, V.P., Sofianos, S.S., Ombao, H., Dybczak, P., Hoteit, I., 2019. Natural climate oscillations may counteract Red Sea warming over the coming decades. Geophys. Res. Lett. 46, 3454–3461. https://doi.org/10.1029/2018GL081397.

Kruskal, W.H., Wallis, W.A., 1952. Use of ranks in one-criterion variance analysis. J. Am. Stat. Assoc. 47, 583–621. https://doi.org/10.2307/2280779.

Legendre, P., Legendre, L., 2012. Numerical Ecology. 3rd edition. Elsevier, Amsterdam, The Netherlands.

Levine, A.F.Z., McPhaden, M.J., Frierson, D.M.W., 2017. The impact of the AMO on multidecadal ENSO variability. Geophys. Res. Lett. 44, 3877–3886. https://doi.org/10.1002/2017GL072524.

Li, A.K., Paek, H., Yu, J.Y., 2016. The changing influences of the AMO and PDO on the decadal variation of the Santa Ana winds. Environ. Res. Lett. 11, 064019. https://doi.org/10.1088/1748-9326/11/6/064019.

Liang, J., Calkin, D.E., Gebert, K.M., Venn, T.J., Silverstein, R.P., 2008. Factors influencing large wildland fire suppression expenditures. Int. J. Wildl. Fire 17, 650–659. https://doi.org/10.1071/WF07010.

Lough, J., Fritts, H., 1987. An assessment of the possible effects of volcanic eruptions on North American climate using tree-ring data, 1602 to 1900 A.D. Clim. Change 10, 219–239.

Maleski, J.J., Martinez, C.J., 2018. Coupled impacts of ENSO AMO and PDO on temperature and precipitation in the Alabama–Coosa–Tallapoosa and Apalachicola–Chattahoochee–Flint river basins. Int. J. Climatol. 38, e717–e728. https://doi.org/10.1002/joc.5401.

Margolis, E.Q., Swetnam, T.W., 2013. Historical fire–climate relationships of upper elevation fire regimes in the south-western United States. Int. J. Wildl. Fire 22, 588–598.

Mariani, M., Fletcher, M., Holz, A., Nyman, P., 2016. ENSO controls interannual fire activity in southeast Australia. Geophys. Res. Lett. 43. https://doi.org/10.1002/2016GL070572.

Mariani, M., Veblen, T.T., Williamson, G.J., 2018. Climate change amplifications of climate-fire teleconnections in the southern climate change amplifications of climate-fire teleconnections in the southern hemisphere. Geophys. Res. Lett. 45. https://doi.org/10.1029/2018GL078294.

Mason, S.A., Hamlington, P.E., Hamlington, B.D., Jolly, M.W., Hoffman, C.M., 2017. Effects of climate oscillations on wildland fire potential in the continental United States. Geophys. Res. Lett. 44, 7002–7010.

Miles, S., Goudey, C., 1997. Ecological Subregions of California: Section and Subsection Descriptions. USDA For. Serv. Pacific Southwest Reg. Publ. R5-EM-TP-0.

Molina-Terrén, D.M., Cardil, A., 2016. Temperature determining larger wildland fires in NE Spain. Theor. Appl. Climatol. 125, 295–302. https://doi.org/10.1007/s00704-015-1511-1.

Molina-Terrén, D.M., Fry, D.L., Grillo, F.F., Cardil, A., Stephens, S.L., 2016. Fire history and management of Pinus canariensis forests on the western Canary Islands Archipelago, Spain. For. Ecol. Manage. 382, 184–192. https://doi.org/10.1016/j.foreco.2016.10.007.

Monedero, S., Ramirez, J., Cardil, A., 2019. Predicting fire spread and behaviour on the fireline. Wildfire analyst pocket: a mobile app for wildland fire prediction. Ecol. Modell. 392, 103–107. https://doi.org/10.1016/j.ecolmodel.2018.11.016.

Moritz, M.A., Parisien, M.A., Batllori, E., Krawchuk, M.A., Van Dorn, J., Ganz, D.J., Hayhoe, K., 2012. Climate change and disruptions to global fire activity. Ecosphere 3, 1–22. https://doi.org/10.1890/ES11-00345.1.

NOAA, 2019. National weather service. Climate prediction center. [WWW document]. URL. https://www.noaa.gov/.

O'Brien, J.P., O'Brien, T.A., Patricola, C.M., Wang, S.-Y.S., 2019. Metrics for understanding large-scale controls of multivariate temperature and precipitation variability. Clim. Dyn. https://doi.org/10.1007/s00382-019-04749-6.

Oksanen, J., Blanchet, F.G., Friendly, M., Kindt, R., Legendre, P., Dan McGlinn, P., Minchin, R., O'Hara, R.B., Simpson, G.L., Solymos, P., Stevens, M.H.H., Szoecs, E., Wagner, H., 2019. Vegan: Community Ecology Package. R Package Version 2.5-6.

Pai Mazumder, D., Jain, P., Done, J., Flannigan, M.D., 2016. Assessing the association of drought to wildfire in California. 30th Conference on Hydrology. American Meteorological Society, New Orleans, LA, US.

Power, S., Delage, F., Chung, C., Kociuba, G., Keay, K., 2013. Robust twenty-first-century projections of El Niño and related precipitation variability. Nature 502, 541–545 Online: https://doi.org/10.1038/nature12580.

Pyne, S., Andrews, P., Laven, R., 1998. Introduction to Wildland Fire. 2nd ed. Wiley, New York.

R core development team, 2017. R 3.2.4.

Ramirez, J., Monedero, S., Silva, C., Cardil, A., 2019. Stochastic decision trigger modelling to assess the probability of wildland fire impact. Sci. Total Environ. 694, 133505. https://doi.org/10.1016/j.scitotenv.2019.07.311.

Schoennagel, T., Veblen, T.T., Romme, W.H., Sibold, J.S., Cook, E.R., 2005. ENSO and PDO variability affect drought-induced fire occurrence in rocky mountain subalpine forests. Ecol. Appl. 15, 2000–2014. https://doi.org/10.1890/04-1579.

Seager, R., Hoerling, M., Schubert, S., Wang, H., Lyon, B., Kumar, A., Nakamura, J., Henderson, N., 2015. Causes of the 2011–14 California drought. J. Clim. 28, 6997–7024. https://doi.org/10.1175/JCLI-D-14-00860.1.

Shabbar, A., Skinner, W., 2004. Summer drought patterns in Canada and the relationship to global sea surface temperatures. J. Clim. 17, 2866–2880.

Skinner, W., Flannigan, M., Stocks, B., Martell, D., Wotton, B., Todd, J., Mason, J., Logan, K., Bosch, E., 2002. A 500 hPa synoptic wildland fire climatology for large Canadian forest fires, 1959–1996. Theor. Appl. Climatol. 71, 157–169.

Sugihara, N., Barbour, M., 2006. Fire and California vegetation. In: Sugihara, N., van Wagtendonk, J., Fites-Kaufman, J., Shaffer, K., Thode, A. (Eds.), Fire in California's Ecosystems. University of California Press, Berkeley, California.

Turco, M., Von Hardenberg, J., AghaKouchak, A., Llasat, M.C., Provenzale, A., Trigo, R.M., 2017. On the key role of droughts in the dynamics of summer fires in Mediterranean Europe. Sci. Rep. 7, 1–10. https://doi.org/10.1038/s41598-017-00116-9.

Vicente-Serrano, S.M., Tomas-Burguera, M., Beguería, S., Reig, F., Latorre, B., Peña-Gallardo, M., Luna, M.Y., Morata, A., González-Hidalgo, J.C., 2017. A high resolution dataset of drought indices for Spain. Data 2, 22. https://doi.org/10.3390/data2030022.

Wang, S., Huang, J., He, Y., Guan, Y., 2014. Combined effects of the Pacific decadal oscillation and El Ninño-southern oscillation on global land dry–wet changes. Sci. Rep. 4, 6651. https://doi.org/10.1038/srep06651.

Westerling, A., Gershunov, A., Brown, T., Cayan, D., Dettinger, M., 2003. Climate and wildfire in the western United States. Bull. Am. Meteorol. Soc. 84, 595–604. https://doi.org/10.1175/bams-84-5-595.

Westerling, A.L., Hidalgo, H.G., Cayan, D.R., Swetnam, T.W., 2006. Warming and earlier spring increase Western U.S. forest wildfire activity. Science 313, 940–943. https://doi.org/10.1126/science.1128834 (80-.).

Williams, A.P., Abatzoglou, J.T., Gershunov, A., Guzman-Morales, J., Bishop, D.A., Balch, J.K., Lettenmaier, D.P., 2019. Observed impacts of anthropogenic climate change on wildfire in California. Earth's Futur. 7, 892–910. https://doi.org/10.1029/2019EF001210.

Yoon, J.-H., Wang, S.-Y.S., Gillies, R.R., Kravitz, B., Hipps, L., Rasch, P.J., 2015. Increasing water cycle extremes in California and in relation to ENSO cycle under global warming. Nat. Commun. 6, 8657. https://doi.org/10.1038/ncomms9657.

Zanchettin, D., Bothe, O., Graf, H., Omrani, N., Rubino, A., Jungclaus, J., 2016. A decadally delayed response of the tropical Pacific to Atlantic Multidecadal Variability. Geophys. Res. Lett. 43, 784–792. https://doi.org/10.1002/2015GL067284.